Bulletin of the Seismological Society of America, Vol. 70, No. 2, pp. 509-527, April 1980

TEMPORAL VARIATION OF SEISMICITY AND SPECTRUM OF SMALL EARTHQUAKES PRECEDING THE 1952 KERN COUNTY, CALIFORNIA, EARTHQUAKE

BY MIZUHO ISHIDA* AND HIROO KANAMORI

ABSTRACT

The spatio-temporal variation of seismicity in the epicentral area of the 1952 Kern County California, earthquake (M_s = 7.7, 34°58.6'N; 119°02'W) was examined for the period prior to the main shock. Most of the events that occurred in the epicentral area were relocated by using the main shock as a master event. A large part of the fault plane of the Kern County earthquake had been seismically quiet for nearly 15 yr before the main shock. However, the activity in the immediate vicinity of the epicenter had been very high during the same period. The temporal variation of the activity in the vicinity of the epicentral area exhibits a pattern very similar to that found for the 1971 San Fernando earthquake. During the 1½ yr period immediately before the main shock, tight clustering of activity around the main-shock epicenter occurred. This clustering may be considered to be foreshock activity. This period of increased activity was preceded by a quiet period for 2 yr from 1949 to 1950; no event was located on the fault plane of the Kern County earthquake during this period. This pattern, quiescence followed by clustering, seems to have repeated several times prior to 1949. Thus, this pattern alone cannot be used as a definite indicator of a large earthquake, but in terms of a fault model with asperities, it can be a manifestation of progressive stress concentration toward the eventual hypocenter. Spectral analyses of the Pasadena Wood-Anderson seismograms of the events that occurred near the epicentral area showed that the frequency of the spectral peak is systematically higher for the foreshocks than the events prior to 1949. A similar trend was found for the 1971 San Fernando earthquake. These results are consistent with the model of stress concentration around the eventual hypocenter.

INTRODUCTION

Spatio-temporal variation of seismicity before large earthquakes has been studied by many investigators in an attempt to understand physical processes leading to an earthquake. The concept of seismic gaps developed by Imamura (1928), Fedotov (1965), Mogi (1968a), Sykes (1971), and Kelleher *et al.* (1973) is fundamental to these recent developments. The most recent review of this subject can be found in McCann *et al.* (1978).

We first review some of the recent progress in this field. Inouye (1965) found that seismicity in the epicentral area of several large earthquakes in Japan (e.g., 1952 Tokachi-Oki earthquake and 1964 Niigata earthquake) had been very low before the main shock. This quiescence was followed by increased activity for several years before the main shock. Inouye also found that the activity in the region surrounding the epicentral area was significantly lower for several months before the main shock. Mogi (1968b) showed that before several large earthquakes (e.g., 1944 Tonankai earthquake and 1946 Nankaido earthquake), the focal region became very calm while the surrounding region was active at the same time. This pattern is often

* Present address: National Research Center for Disaster Prevention, Science and Technology Agency, Ibaraki, Japan.

called a doughnut pattern. A similar doughnut pattern has been found for a magnitude 6 earthquake in Kyushu, Japan by Mitsunami and Kubotera (1977), and for a magnitude 6.1 earthquake in the Shimane prefecture, Japan by Yamashina and Inoue (1979). Various space-time patterns of large earthquakes in the Japanese region have been discussed in detail by Utsu (1968, 1974). In the case of the recent Oaxaca, Mexico earthquake (November 29, 1978, $M_s = 7.5$ to 7.8), its magnitude and location came very close to those predicted by Ohtake *et al.* (1977) who used a preseismic quiescence in the epicentral area as the primary basis of their prediction. Although some of the details of this prediction remain to be investigated (Singh *et al.*, 1979), Ohtake *et al.* (1977) made a good case that the spatio-temporal pattern of seismicity is indeed a powerful tool for long-term prediction of earthquakes.

Kelleher and Savino (1975) demonstrated that gaps in seismicity for great earthquakes along major plate boundaries are also gaps for smaller magnitude activity and such gaps commonly persist until the time of the main shock. They noted that seismic activity before the main shock frequently occurred near the epicenter of the main shock and/or near the edges of the rupture zone.

Another important feature is a clustering of seismic activity. McNally (1980) found that distinct clusters of small earthquakes occurred in the near-source region of several moderate size earthquakes in Central California 2 to 10 yr before the main shock. Sekiya (1976, 1977), and Ohtake (1976), reported that anomalous seismic activity occurred about 10 yr before the 1974 Izu-Hanto-Oki earthquake in the epicentral area which had been generally very quiet before the earthquake. Sekiya (1977) reported similar examples for about ten other Japanese earthquakes. Evison (1977a, b) found such precursory activities before the 1968 Borrego Mountain, California earthquake, and several earthquakes in New Zealand, including the 1966 Gisborne earthquake, the 1968 Inangahua earthquake, and the 1976 Milford Sound earthquake. Evison (1977a) considered that a burst of seismic activity marks the start of a precursory sequence, and called it the precursory earthquake swarm. This precursory swarm is often followed by a period of abnormal quiescence which lasts until the onset of the major event. In the studies of Evison (1977a, b), Sekiya (1977), and Ohtake (1976), the precursory swarm is not necessarily considered to have occurred in the immediate vicinity of the epicenter. The epicenters of the swarm events are sometimes distributed widely in the eventual aftershock area and its surroundings. For the earthquakes studied by these authors, the activity of immediate foreshocks was not always evident. Brady (1976) found a clustering of seismic activity before the 1971 San Fernando, California earthquake and interpreted it as a primary inclusion zone of the impending failure.

In these studies, there are three important elements: (1) preseismic quiescence in the epicentral area; (2) a precursory swarm (not immediate foreshocks); (3) change in seismicity in the surrounding area [increase (Mogi, 1969) or decrease (Inouye, 1965)]. Another important element is a clustering of activity immediately before the main shock. Mogi (1968c) and Kelleher and Savino (1975) demonstrated that seismic activity prior to a great earthquake tends to cluster around the epicenter of the eventual main shock. More recently, Ishida and Kanamori (1977, 1978) and Fuis and Lindh (1979) found a very tight clustering of activity before the 1971 San Fernando, California, and the 1975 Galway Lake, California, earthquakes, respectively. The clustering for the San Fernando earthquake occurred during the 2-yr period before the main shock. This clustering followed a period of quiescence which had lasted for 4 yr, and can be considered to be foreshock activity.

Engdahl and Kisslinger (1977) also found small foreshocks before a magnitude 5 earthquake in the Central Aleutians. They reported that six small earthquakes followed a period of decreased seismicity in the epicentral area and migrated toward the location of the main event.

However, despite these findings, it is not yet clear whether there is any universal precursory seismicity pattern which can be used for definitive prediction purposes. Foreshock activity is the most distinct among all the patterns discussed above, but it is often difficult to distinguish the foreshock activity from the background activity. In the cases of the 1975 Galway Lake earthquake, the 1971 San Fernando earthquake, and the 1976 Adak Island earthquake, the foreshock activity was rather distinct in two respects. First, it was preceded by a very quiet period and, second, they were very tightly clustered near the epicenter of the main shock. However, as will be shown later, a closer examination of the San Fernando data reveals that this pattern, quiescence followed by increased activity, repeated itself several times in the past. A question is then raised as to how we can distinguish the last sequence from the earlier ones. Ishida and Kanamori (1978) suggested a method for identifying a foreshock sequence through detailed analyses of waveforms, spectra, and mechanism. In the present study, we apply this method to the 1952 Kern County,

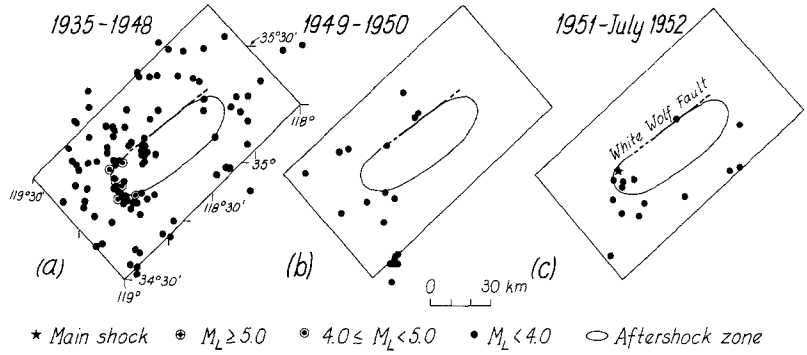

FIG. 1. Spatial distribution of relocated epicenters before the 1952 Kern County earthquake for three periods.

California, earthquake ($M_s = 7.7$), the largest earthquake in California since 1906, in an attempt to better understand the nature of the seismicity pattern, especially for major California earthquakes.

SEISMICITY PATTERNS

In this paper we investigate seismicity in a 67 × 124 km^2 rectangular area surrounding the White Wolf Fault and the aftershock area of the 1952 Kern County earthquake (Figure 1). A few events which occurred within 30 km of this rectangular area are included in the analysis.

Most of the events which occurred in the study area during the period from 1933 to the occurrence of the 1952 Kern County earthquake were relocated by using the main shock as a master event. The method of relocation is essentially the same as that employed by Hadley and Kanamori (1978) and Ishida and Kanamori (1978). The HYPO 71 location program (Lee and Lahr, 1975) was used and the S-P times at stations within 200 km from the epicenter were included in the analysis. The P and S times registered in the original card file at the Seismological Laboratory and the crustal structure employed by Hadley and Kanamori were used. Some of the

events could not be relocated because the data are too sparse or the phase cards are missing in the card file. The details are given in Table A-1 of the Appendix.

Although the absolute accuracy of the hypocentral location is difficult to estimate, the relative locations are probably accurate to ±10 km. Furthermore, relocation by the same method removes a possible bias which may have been caused by changes in the location method over the years from 1933 to 1952. We believe that these relocated epicenters give a better picture of the seismicity pattern of the area than that obtained from the published catalog (Hileman *et al.*, 1973). The hypocentral parameters of the relocated events are listed in Table A-1 in the Appendix.

Figure 1 shows the distribution of epicenters before the 1952 Kern County earthquake for three periods thus obtained. A large part of the fault plane of the

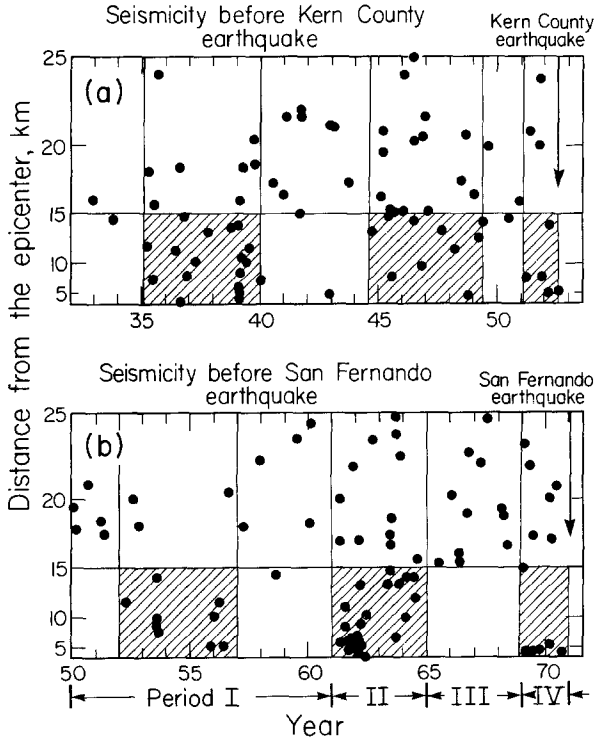

FIG. 2. The distance L between the epicenter of the main shock and the individual event as a function of year for the 1952 Kern County earthquake (a) and for the 1971 San Fernando earthquake (b). The length of the ordinate is taken proportional to L^2.

Kern County earthquake had been seismically quiet for nearly 15 yr before the main shock. However, the activity in the immediate vicinity of the epicenter was relatively high during the same period as shown in Figure 2a, in which the distance L between the epicenter of the main shock and the individual events is plotted as a function of time. This pattern of seismicity has already been noted by Wesson and Ellsworth (1973) and Kelleher and Savino (1975). The temporal variation of the activity around the epicenter exhibits a pattern very similar to that found for the 1971 San Fernando earthquake (Figure 2b). During the $1\frac{1}{2}$ yr period immediately before the main shock, a tight clustering of activity around the main shock epicenter occurred. This clustering may be considered to be a foreshock activity. This period was

preceded by a quiet period for about 2 yr from 1949 to 1950; no event was located on the eventual fault plane of the Kern County earthquake during this period.

In order to examine the background activity near the epicentral area in more detail, seismicity during the period from 1933 to 1950 was divided into consecutive 2-yr periods. Each figure of Figure 3a presents seismicity for each 2-yr period, except the last one which represents the period from January 1951 to July 21, 1952, the time of the main shock. The pattern, quiescence followed by a clustering, seems to have repeated several times prior to 1949 [e.g., 1933 to 1934 (quiescence) followed by 1935 to 1936 (clustering), 1937 to 1938 (quiescence) followed by 1939 to 1940 (clustering), and 1941 to 1944 (quiescence) followed by 1947 to 1948 (clustering)].

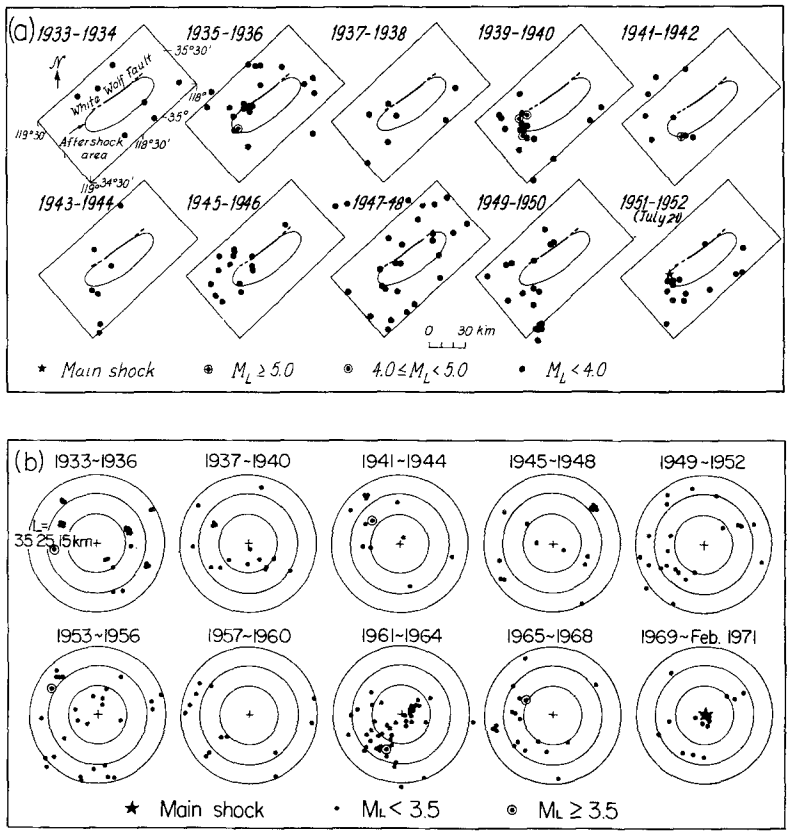

FIG. 3. (a) Seismicity in the epicentral area of the 1952 Kern County earthquake for consecutive 2-yr periods, except the last figure that represents the period from January 1951 to July 1952. (b) Seismicity in the epicentral area of the 1971 San Fernando earthquake as a function of time. Each figure represents seismicity for consecutive 4-yr periods, except the last figure that represents the period from January 1969 to February 1971.

A similar pattern of repetition was also found for the 1971 San Fernando earthquake (Figures 2b and 3b). In particular, the quiet period from 1957 to 1960 was followed by very active clustering during the period from 1961 to 1962 (see Figure 2b). If this type of seismicity pattern had been identified in 1962, this clustering would have been erroneously identified as foreshock activity. Thus, the seismicity pattern alone cannot be used as a definite indicator of a large earthquake.

In this study, spectral characteristics of the events which occurred in the main shock epicentral area were investigated to see whether the clustering activity just before the main shock is distinguishable from the earlier ones.

Spectral Analysis

For the study of frequency spectra of seismic events, seismograms recorded by a broad-band instrument are most suitable. In this paper, the records of the standard Wood-Anderson seismographs were used, which have an essentially flat displacement response over the period range of our interest. About six stations of the seismographic network of the California Institute of Technology were operating

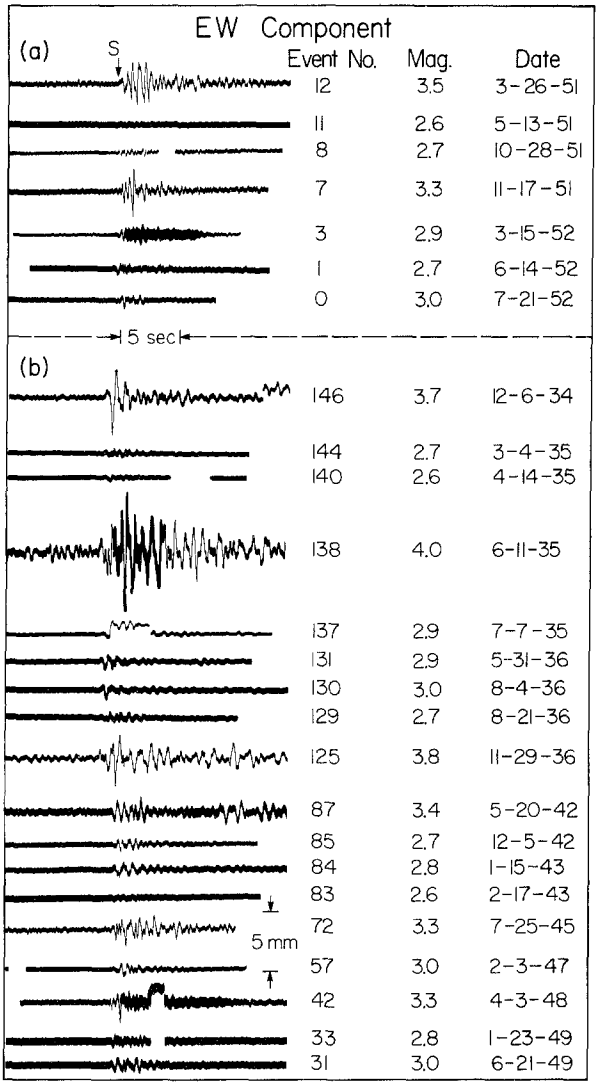

FIG. 4. The EW component Wood-Anderson seismograms of the S waves from the events near the epicenter recorded at Pasadena for the period 1951 to 1952 (foreshocks) (a) and 1934 to 1949 (b). The event numbers refer to those of Table A-1.

Wood-Anderson seismographs prior to the 1952 Kern County earthquake. Among these, the Pasadena station which is located at a reasonably short distance ($\Delta \sim 120$ km) from the epicenter maintained the operation of the Wood-Anderson seismographs during the entire period from 1933 to 1952 on a uniform basis.

Figures 4 and 5 show the S waves recorded on the Wood-Anderson seismograms at Pasadena. All the available records of the events with $2.6 < M_L < 4.0$ that

occurred in the immediate vicinity of the epicenter of the Kern County earthquake are shown. The seismograms of the events during the period from 1934 to 1949 are shown in Figures 4b and 5b. Ishida and Kanamori (1978) found that the waveforms of the foreshocks of the 1971 San Fernando earthquake are very different from that of the events during other periods. The foreshocks of the San Fernando earthquake are very complex, yet remarkably similar to each other. For the Kern County earthquake, the difference in the waveform between the foreshocks and other events

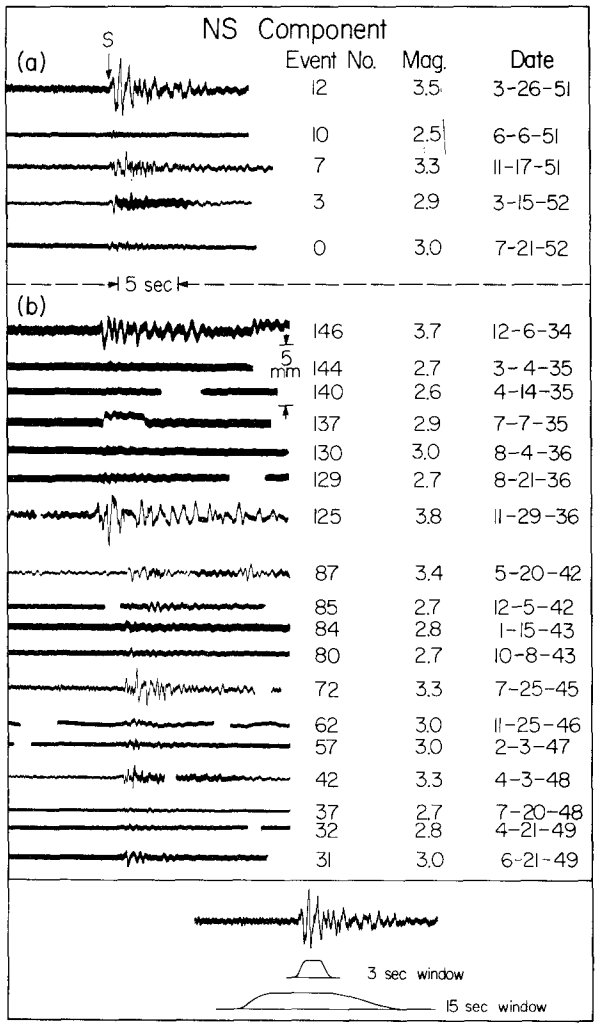

FIG. 5. The NS component Wood-Anderson seismograms of the *S* waves from the events near the epicenter recorded at Pasadena for the period 1951 to 1952 (foreshocks) (a) and 1934 to 1949 (b). The event numbers refer to those of Table A-1. The figure at the *bottom* illustrates the 3-sec and the 15-sec windows and the tapering used in the analysis.

is not obvious. Furthermore, the waveform of the foreshocks varies substantially from event to event.

In order to investigate whether there is any significant difference in the frequency content between the foreshocks and other events, spectral analyses of these seismograms were performed. The first 3 sec of the *S*-wave trains were windowed, cosine-tapered (33 per cent in the beginning and at the end), as illustrated at the bottom of Figure 5, and used for the analysis. Figures 6 and 7 show the amplitude

spectral densities of the seismograms shown in Figures 4 and 5. The arrow in each figure shows the spectral peak that was identified. When more than one peak occurred with approximately equal strength (e.g., events 1 EW, 144 EW), the average frequency of these peaks was used. As shown by Figure 8, the frequency of the

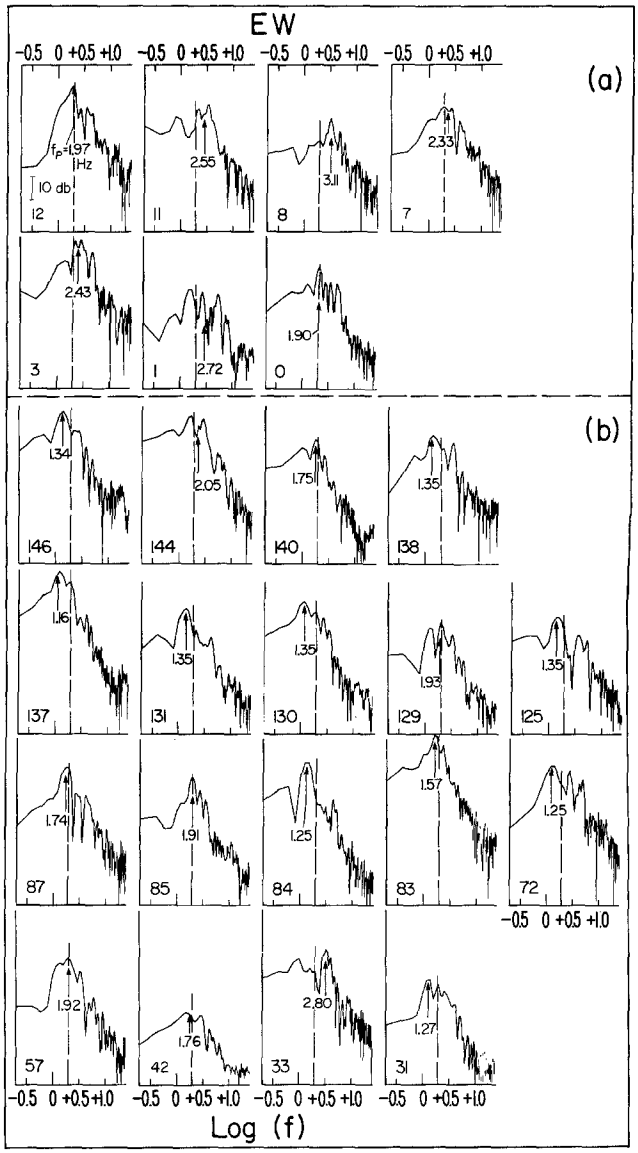

FIG. 6. The *S*-wave amplitude spectra of the EW component Wood-Anderson seismograms. The event numbers correspond to those of Figure 4 and Table A-1. The arrows indicate the frequency at the peak amplitude. The events for the period 1951 to 1952 (foreshocks) and 1934 to 1949 are shown in (a) and (b), respectively. Dashed lines are drawn as reference at 1.9 Hz. Note that the spectral peak of most of the foreshocks is located to the *right* of the reference line, and that for the events prior to 1950, to the *left*.

spectral peak is systematically higher than 2.2 Hz for the foreshocks (except event 12) while that of other events (except event 33) is lower than 2.2 Hz.

Because of the finite line thickness of the optical recording, the time marks and other signal-generated noises, the signal-to-noise ratio of these records is not very

high. In order to see the signal-to-noise ratio, the noise spectra for three representative records were computed, 12 EW (good quality), 7 EW (good quality), and 11 EW (poor quality), and were compared with the signal spectra. A 3-sec record starting 5.6 sec after the onset of the S arrival was taken as the noise. The spectra are shown in Figure 9. For the records, 12 EW and 7 EW, the signal spectral density

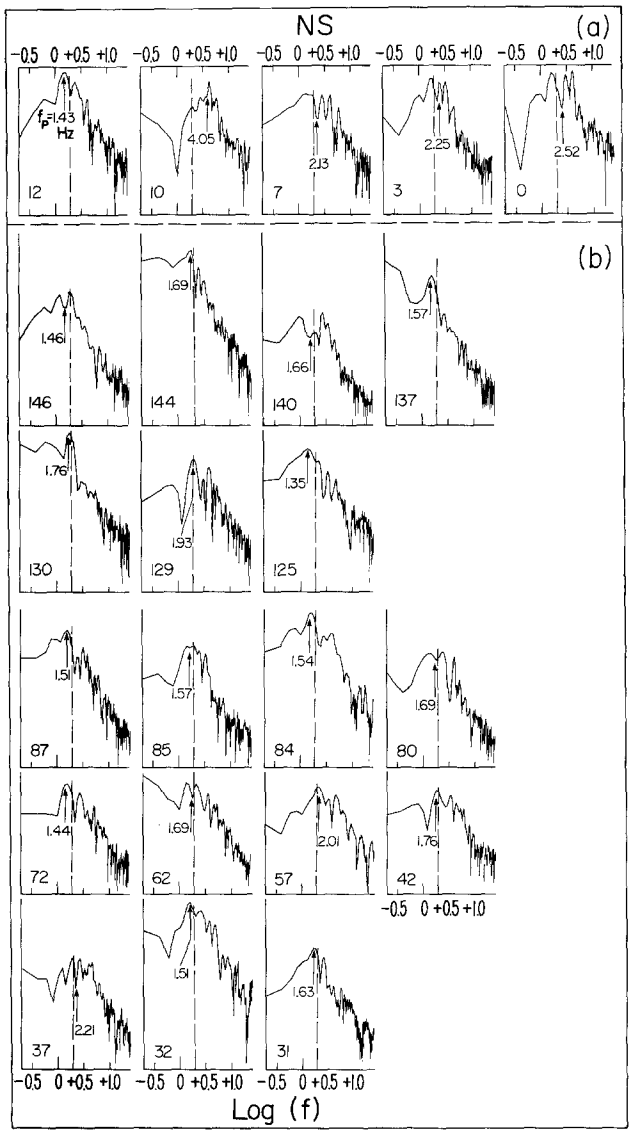

FIG. 7. The S-wave amplitude spectra of the NS component Wood-Anderson seismograms. The event numbers correspond to those of Figure 5 and Table A-1. The arrows indicate the frequency at the peak amplitude. The events for the period 1951 to 1952 (foreshocks) are shown in (a) and those from 1934 to 1949 in (b).

is about 10 dB above the noise over the frequency range of our interest (i.e., 1 to 10 Hz). For the record 11 EW, the noise level, is comparable to the signal at frequencies lower than 1.5 Hz, but the signal level is considerably higher than the noise level near the peak frequency. The record 11 EW is the worst record used in this paper and the significance of the result obtained from this record should be considered

marginal. However, it is thought that the results obtained from other records are significant at frequencies lower than 10 Hz.

In order to examine the effect of the window length on the position of the spectral peak, a similar analysis was performed by using a much longer, 15-sec record that includes the *S*-wave energy. Since most of the energy is contained in the first 3 sec of the *S*-wave train, the result remained essentially the same.

The frequency content of the events is determined by many factors such as the stress in the focal zone, the source dimension, the structure of the medium, the depth of the events, and the focal mechanism. Unfortunately, because of the sparse distribution of the stations prior to 1952, the depth and the focal mechanism of

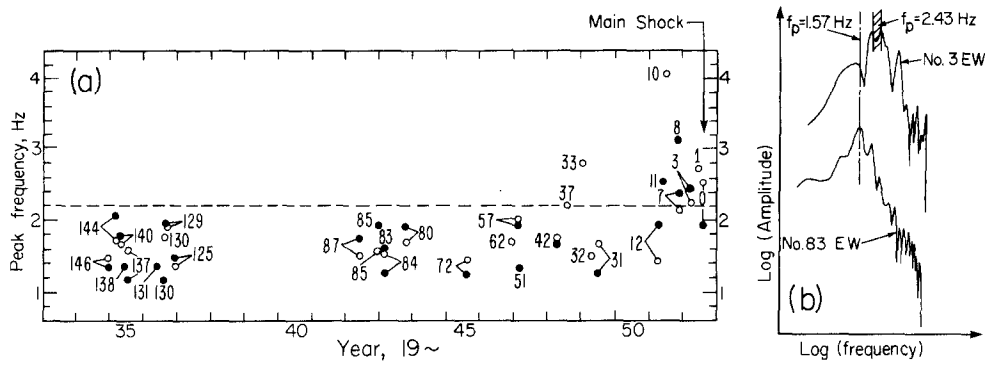

FIG. 8. The variation of peak frequency as a function of time. Closed circles show the EW components and open circles the NS components. Note the shift of the frequency during the period from 1951 to July 1952. The figure to the *right* illustrates the difference between events 3 and 83.

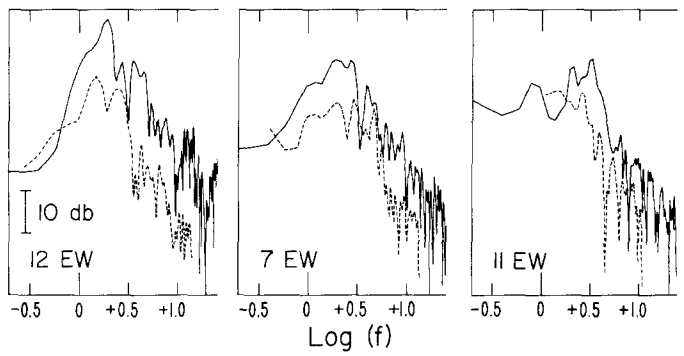

FIG. 9. Comparison of signal and noise spectra. The signal and noise are taken from a 3-sec record starting from the beginning and 5 to 6 sec after the onset of the *S* phase, respectively.

these events could not be determined. The source dimension of the events may be inferred from the magnitude. By using the relation obtained by Wyss and Brune (1968), the source dimension of the events (M_L = 2.6 to 4.0) used in this analysis can be estimated to be from 0.8 to 4.3 km. Since the corresponding corner frequencies are between 0.6 and 3 Hz, Figure 8 may contain the effect of the variation of the magnitude of the events used. In order to examine this effect, the frequency of the spectral peak is plotted in Figure 10 as a function of the magnitude. Since the magnitude, M_L, listed in the Caltech catalog (Hileman *et al.*, 1973) for most of the events prior to 1944 is given only to the nearest 0.5 unit, M_L of all the events used for this comparison were recalculated by using the amplitude data listed on the

event cards in the Caltech file. The recalculated values of M_L for these events are entered in Table A-1. Although a slight trend of decreasing peak frequency with increasing magnitude is seen, the peak frequency of the foreshocks is always higher than that of other events for each magnitude range. Hence, it is concluded that the difference in the magnitude is not the cause of the major feature of Figure 8.

The effect of the stress in the focal zone on the frequency content of an event is not well understood. In terms of a very simple source model such as the one developed by Brune (1970), the high-frequency end of the seismic spectrum is controlled by the effective tectonic stress (dynamic stress drop) which is likely to be proportional to the *in situ* stress in the focal zone. Although the actual process is probably more complex than Brune's (1970) model, especially at high frequencies, events with more high-frequency energy may be expected as the tectonic stress becomes higher, if other conditions remain the same.

The idea of using spectral characteristics to estimate the dynamic stress drop has been used by a number of investigators (e.g., Brune, 1970; Wyss and Brune, 1968).

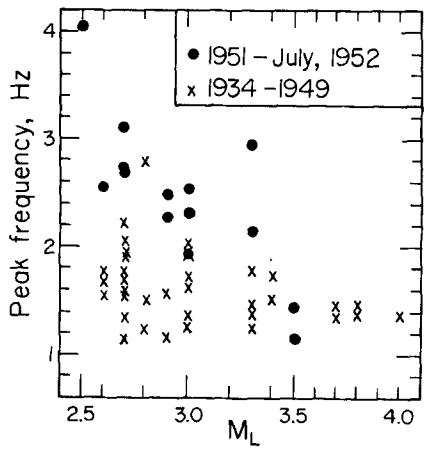

FIG. 10. The peak frequency as a function of magnitude. Closed circles show the foreshocks and crosses show the events for the period 1934 to 1949.

Archambeau (1978) used a stress-relaxation source model to estimate the level of dynamic stress drop along various subduction zones. House and Boatwright (1978) reported two very high-stress drop events in the Shumagin seismic gap, Alaska, and suggested a possibility of considerable stress accumulation in this gap.

Clustering of micro-cracks on the eventual failure zone has already been noticed by Mogi (1968c) and Scholz (1968) in laboratory experiments. A recent study by Kusunose (1977) demonstrated that the waveforms of elastic shocks in a rock specimen contained high-frequency oscillations under high-stress level prior to a major failure. These laboratory experiments suggest that tight clustering and shift of the spectral peak toward high frequency before a large earthquake may be a common feature.

In view of the result of these investigations, the preferred interpretation is that the observed increase in the peak frequency during the foreshock period is primarily a result of increased stress near the hypocenter. Unfortunately, no more data are available to supplement the data shown in Figure 8. Another station which operated the Wood-Anderson seismograph is located at Santa Barbara ($\Delta \cong 100$ km), but the records are too incomplete to be used for the present study. Other stations are too

far away from the epicenter to record the small events in the epicentral area of the Kern County earthquake.

In order to compare the Kern County earthquake with the San Fernando earthquake, the same analysis was performed on the Wood-Anderson seismograms of the San Fernando earthquake. The results are shown in Figure 11. The seismo-

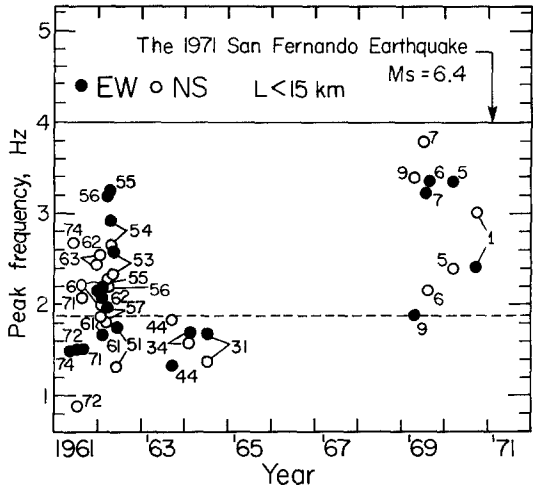

FIG. 11. The peak frequency as a function of time for the 1971 San Fernando earthquake. Note the lack of low-frequency events during the foreshock period.

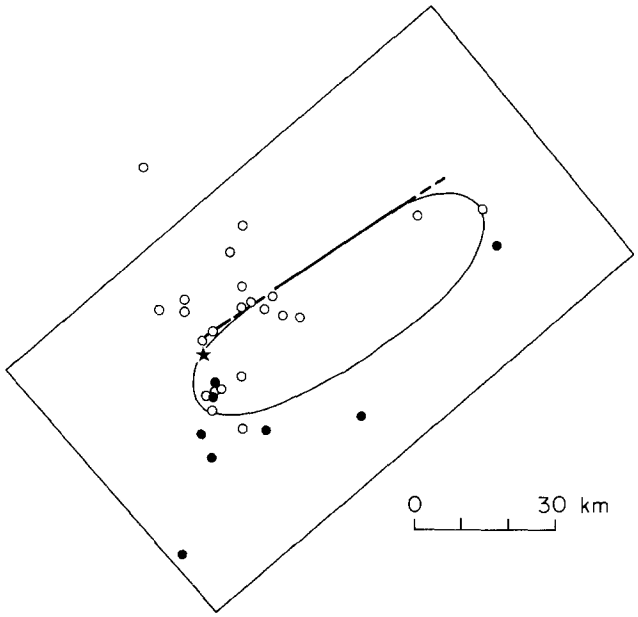

FIG. 12. Location of the high-frequency events (events with the peak frequency higher than 2.2 Hz) and the low-frequency events. Closed circles: high-frequency events; open circles: low-frequency events.

grams used for this analysis are shown in Figures 2 and 3 of Ishida and Kanamori (1978). Figure 11 clearly indicates that the foreshocks invariably show high-peak frequencies, while the activity prior to 1964 includes both high-frequency and low-frequency events. The lack of low-frequency events during the foreshock sequence appears to be an important feature of Figure 11.

It is possible that there is a systematic difference between the locations, both horizontally and vertically, of the foreshocks and the earlier activity. The observed difference in the peak frequency may be due to this migration of the events, rather than the direct effect of stress changes. Figure 12 shows the spatial distribution of the high-frequency and the low-frequency events. It is interesting to note that all the high-frequency events occurred to the south of the White Wolf Fault, in the hanging wall block. However, a significant number of low-frequency events occurred in the same block, and no obvious separation between the high-frequency and the low-frequency events is seen. The data set for the Kern County earthquake is admittedly too incomplete, in both quality and quantity, to resolve further details.

Furthermore, whether foreshocks are always higher frequency events or not is still unresolved. Bakun and McEvilly (1979) conclude that, for the 1966 Parkfield earthquake and the 1975 Oroville, California, earthquake foreshock radiation is neither universally higher nor lower frequency than comparable normal earthquakes. However, it is encouraging that the present results strongly suggest that measurements with better instrumentation (wide-band, wide dynamic range) at a short distance can distinguish foreshock activity from the background activity on the basis of spectra.

Conclusion and Discussion

As Kelleher and Savino (1975) and Wesson and Ellsworth (1973) have pointed out, seismicity in the immediate vicinity of the epicenter of the 1952 Kern County earthquake was considerably higher than in the surrounding area before the main shock. A more detailed inspection of this activity revealed a period of very low activity from 1949 to 1950 which was followed by foreshock activity, increased activity for the $1\frac{1}{2}$-yr period just before the main shock. This pattern, quiescence followed by increased activity in the immediate vicinity of the eventual main shock epicenter, is similar to that found for several other earthquakes, especially the 1971 San Fernando and the 1976 Adak Island earthquake. However, this pattern had repeated at least several times during the 20-yr and the 40-yr periods before the Kern County and the San Fernando earthquakes, respectively. Thus, the seismicity pattern alone cannot be used as a definite indicator of a large earthquake. The most encouraging result of the present study is the temporal change in the waveform and the frequency content of the events which occurred in the epicentral area. The results for both the Kern County and the San Fernando earthquakes suggest that the foreshocks had consistently higher peak frequencies than other events.

Unfortunately, the distance to the station used in the present study is very large, especially for the Kern County earthquake, so that most high-frequency (e.g., higher than several Hz) energy is lost during the propagation. Nevertheless, the change is still recognizable in Figures 6 and 7. If several broad-band stations were operated in the epicentral area, the change would have been detected more unambiguously.

At present, there is no established physical model linking such clusterings to the occurrence of the eventual main shock. A very simple, yet plausible, model is the asperity model such as the one discussed by Ishida and Kanamori (1978) and Kanamori (1978). At the earlier stage of an earthquake preparatory process, the stress distribution on the fault plane is characterized by a more or less uniform distribution of small asperities. As the tectonic stress increases, weaker asperities break in the form of background small earthquakes. Eventually, only strong asperities remain unbroken. Seismic activity occurs only around these asperities as

occasional clusterings of earthquakes, leaving the surrounding area seismically quiet. Eventually only the strongest asperity is left unbroken. As the stress builds up around this asperity, very tightly clustered activity sporadically occurs there, while the rest of the fault plane remains quiet. The frequently observed seismicity pattern, quiescence followed by a clustering, may correspond to this stage. When the stress around this asperity reaches the ultimate strength of the asperity, the final failure, the main shock, occurs. Small earthquakes preceding this event contain very high frequency waves reflecting the high local stress concentration. Although further investigation is clearly necessary before a more concrete model can be constructed, the present result demonstrates that with a long-term (20 to 40 yr) data base with uniform quality, seismological techniques can be used to monitor spatio-temporal changes of stress distribution on the fault plane. This information is believed to be fundamental to a better understanding of earthquake failure process and to an implementation of reliable earthquake prediction method.

Acknowledgments

We thank Kazuya Fujita, Tracy Johnson, and Don Anderson for valuable comments.

This research was funded by U.S. Geological Survey Contract 14-08-0001-17631. Mizuho Ishida was partially supported by a fellowship from the Science and Technology Agency in Japan.

References

Archambeau, C. (1978). Estimation of non-hydrostatic stress in the Earth by seismic methods: lithospheric stress levels along Pacific and Nazca plate subduction zones, Proc. of Conf. VI, Methodology for identifying seismic gaps and soon-to-break gaps, *U.S. Geol. Surv., Open-File Rept. 78-943,* 47–138.

Bakun, W. H. and T. V. McEvilly (1979). Are foreshocks distinctive? Evidence from the 1966 Parkfield and the 1975 Oroville, California sequences, *Bull. Seism. Soc. Am.* **69,** 1027–1038.

Brady, B. T. (1976). Theory of earthquakes, IV, *Pure Appl. Geophys.* **114,** 1031–1082.

Brune, J. N. (1970). Tectonic stress and the spectra of seismic shear waves from earthquakes, *J. Geophys. Res.* **75,** 4997–5009.

Engdahl, E. R. and C. Kisslinger (1977). Seismological precursors to a magnitude 5 earthquake in the Central Aleutian Islands, *J. Phys. Earth* **25,** S243–S250.

Evison, F. F. (1977a). Fluctuations of seismicity before major earthquakes, *Nature* **266,** 710–712.

Evison, F. F. (1977b). Precursory seismic sequences in New Zealand, *New Zealand J. Geol. Geophys.* **20,** 129–141.

Fedotov, S. A. (1965). Regularities of the distribution of strong earthquakes in Kamchatka, the Kuril islands and northeastern Japan, *Trudy Inst. Fiz. Zemli* **36,** 66–93 (in Russian).

Fuis, G. S. and A. G. Lindh (1979). A change in fault-plane orientation between foreshocks and aftershocks of the Galway Lake earthquake, $M_L = 5.2$, 1975, Mojave Desert, California (abstract), *Tectonophysics* **52,** 601–602.

Hadley, D. and H. Kanamori (1978). Recent seismicity in the San Fernando region and tectonics of the west-central Transverse Ranges, California, *Bull. Seism. Soc. Am.* **68,** 1449–1457.

Hileman, J. A., C. R. Allen, and J. M. Nordquist (1973). Seismicity of the Southern California region, 1 January 1932 to 31 December 1972, Seismological Laboratory, California Institute of Technology, Pasadena, 83 pp.

House, L. and J. Boatwright (1978). Investigation of two high stress-drop earthquakes in the Shumagin seismic gap, Alaska, *EOS* **59,** 1124.

Imamura, A. (1928). On the seismic activity of central Japan, *Jap. J. Astron. Geophys.* **6,** 119–137.

Inouye, W. (1965). On the seismicity in the epicentral region and its neighborhood before the Niigata earthquake, *Kenshin Jiho* **29,** 31–36 (in Japanese).

Ishida, M. and H. Kanamori (1978). The foreshock activity of the 1971 San Fernando earthquake, California, *Bull. Seism. Soc. Am.* **68,** 1265–1279.

Kanamori, H. (1978). Use of seismic radiation to infer source parameters, Proc. of Conf. IV, Fault Mechanics and Its Relation to Earthquake Prediction, *U.S. Geol. Surv., Open-File Rept. 78-380,* 283–317.

Kelleher, J., L. Sykes, and J. Oliver (1973). Possible criteria for predicting earthquake locations and their application to major plate boundaries of the Pacific and the Caribbean, *J. Geophys. Res.* **78,** 2547–2585.

Kelleher, J. and J. Savino (1975). Distribution of seismicity before large strike-slip and thrust-type earthquakes, *J. Geophys. Res.* **80,** 260–271.

Kusunose, K. (1977). Source process of acoustic emissions in rocks under uniaxial compression, *Ph.D. Dissertation,* Tohoku University, Japan, 121 pp. (in Japanese).

Lee, W. H. K. and J. C. Lahr (1975). HYPO71 (Revised), A computer program for determining hypocenter, magnitude and first motion pattern of local earthquakes, *U.S. Geol. Surv., Open-File Rept. 75-311,* Washington, D.C., 113 pp.

McCann, W. R., S. P. Nishenko, L. R. Sykes, and J. Krause (1978). Seismic gaps and plate tectonics: seismic potential for major plate boundaries, Proc. of Conf. VI, Methodology for identifying seismic gaps and soon-to-break gaps, *U.S. Geol. Surv., Open-File Rept. 78-943,* 441–584.

McNally, K. C. (1980). Patterns of earthquake clustering preceding moderate earthquakes, Central California, submitted for publication.

Mitsunami, T. and A. Kubotera (1977). On the activity of the earthquake swarm in the northern part of Aso Caldera, 1975—Interpretation of hypocentral migration, *Zisin* **30,** 73–90.

Mogi, K. (1968a). Sequential occurrence of recent great earthquakes, *J. Phys. Earth* **16,** 30–36.

Mogi, K. (1968b). Some features of recent seismic activity in and near Japan, 1, *Bull. Earthquake Res. Inst., Tokyo Univ.* **46,** 1225–1236.

Mogi, K. (1968c). Source locations of elastic shocks in the fracturing process in rocks (I), *Bull. Earthquake Res. Inst., Tokyo Univ.* **46,** 1103–1125.

Mogi, K. (1969). Some features of recent seismic activity in and near Japan, 2, *Bull. Earthquake Res. Inst., Tokyo Univ.* **47,** 395–417.

Ohtake, M. (1976). Search for precursors of the 1974 Izu-hanto-oki earthquake, Japan, *Pageoph* **114,** 1083–1093.

Ohtake, M., T. Matsumoto, and G. V. Latham (1977). Seismicity gap near Oaxaca, southern Mexico as a probable precursor to a large earthquake, *Pageoph* **115,** 375–385.

Scholz, C. H. (1968). Experimental study of the fracture process in brittle rock, *J. Geophys. Res.* **73,** 1447–1454.

Sekiya, H. (1976). The seismicity preceding earthquakes and its significance to earthquake prediction, *J. Seism. Soc., Japan* **25,** 299–311 (in Japanese).

Sekiya, H. (1977). Anomalous seismic activity and earthquake prediction, *J. Phys. Earth* **25,** (*Suppl.*), S85–S93.

Singh, S. K., J. Havskov, K. McNally, L. Ponce, T. Hearn, and M. Vassiliou (1979). The Oaxaca, Mexico, earthquake of 29 November 1978: A preliminary report on aftershocks, submitted for publication.

Sykes, L. R. (1971). Aftershock zones of great earthquakes, seismicity gaps, and earthquake prediction for Alaska and the Aleutians, *J. Geophys. Res.* **76,** 8021–8041.

Utsu, T. (1968). Seismic activity in Hokkaido and its vicinity, *Geophys. Bull. Hokkaido Univ.* **20,** 51–75 (in Japanese).

Utsu, T. (1974). Space-time pattern of large earthquakes occurring off the coast of the Japanese islands, *J. Phys. Earth* **22,** 325–342.

Wesson, R. L. and W. L. Ellsworth (1973). Seismicity preceding moderate earthquake in California, *J. Geophys. Res.* **78,** 8527–8546.

Wyss, M. and J. N. Brune (1968). Seismic moment, stress and source dimension for earthquakes in the California-Nevada region, *J. Geophys. Res.* **73,** 4681–4694.

Yamashina, K. and Y. Inoue (1979). A doughnut-shaped pattern of seismic activity preceding the Shimane earthquake of 1978, Japan, *Nature* **278,** 48–50.

SEISMOLOGICAL LABORATORY
CALIFORNIA INSTITUTE OF TECHNOLOGY
PASADENA, CALIFORNIA 91125
CONTRIBUTION NO. 3216

Manuscript received May 16, 1979

APPENDIX

TABLE A-1

HYPOCENTER PARAMETERS OF RELOCATED EVENTS

		Lat (N)	Long (W)
Area		35°42.0′	118°30.0′
		35°15.0′	118° 6.0′
		34°30.0′	119° 0.0′
		34°57.0′	119°30.0′
Period		1932 to July 21, 1952	
Master event: Kern County Earthquake			

No.	Y	M D	H M	Sec	Lat (N)	Long (W)	M_L (M_S)
	'52	7 21	11 52	14.45	34° 58.6′	119° 2.0′	7.7
0*		7 21	9 43	4.28	34 55.7	119 0.3	3.0
1*		6 14	16 54	51.53	34 52.0	118 40.0	2.7
2*		4 13	7 47	6.57	34 51.0	119 3.7	2.5
3*		3 15	6 44	47.78	34 36.3	119 4.7	2.9
4*		3 7	23 23	41.98	34 54.0	119 3.5	2.5
5	'51	12 28	8 23	57.77	35 0.1	118 21.7	3.1
6		12 26	3 12	39.47	34 46.7	118 55.0	2.8
7*		11 17	4 20	28.66	34 54.1	119 0.6	3.3
8*		10 28	7 19	33.51	34 50.1	118 53.4	2.7
9*		8 18	0 6	38.39	34 12.1	118 42.4	2.6
10*		6 6	2 47	51.22	34 47.2	119 0.9	2.5
11		5 13	2 19	22.04	35 11.1	118 21.3	2.6
12*		3 26	0 25	56.78	34 56.3	118 57.1	3.5
13		1 19	17 48	52.38	34 59.0	118 25.0	3.2
14	'50	12 17	18 58	51.44	34 44.3	118 56.6	2.5
15		12 14	13 56	23.02	35 2.7	119 11.4	4.4
16		11 28	8 33	48.44	34 57.1	119 22.3	2.8
17		11 11	19 32	28.83	34 33.7	118 52.1	3.1
18			19 27	22.53	34 36.0	118 51.9	2.7
19			19 14	39.59	34 35.7	118 52.1	3.3
20		11 4	0 47	45.28	35 13.0	118 45.0	2.5
21		11 2	6 39	26.07	35 18.5	118 50.0	2.6
22		10 11	7 46	33.19	34 34.5	118 52.9	2.3
23		6 30	19 31	11.28	34 52.0	118 56.0	2.5
24		3 23	10 52	49.67	35 5.5	118 16.1	3.0
25		2 10	22 38	57.76	35 12.0	118 46.0	2.7
26		1 27	15 1	26.46	34 33.9	118 54.0	2.6
27		1 25	10 34	2.43	34 29.0	118 53.4	3.1
28		1 24	21 57	0.44	34 33.7	118 52.9	4.0
29	'49	7 29	8 35	19.88	34 50.4	118 53.0	2.8
30		7 14	8 14	35.30	34 46.5	119 10.7	3.0
31		6 21	22 8	18.17	35 4.3	118 55.3	3.0
32		4 21	7 12	22.0	35 3.6	119 8.5	2.8
33		1 23	4 38	43.44	34 49.8	119 2.1	2.8
34	'48	10 28	2 27	5.92	35 1.0	119 2.0	2.8
35		9 16	17 48	14.99	34 50.7	118 52.2	3.0
36		9 16	11 26	33.58	34 33.9	118 58.4	2.7
37		7 20	9 35	42.76	35 3.2	118 51.5	2.7
38		5 31	19 9	27.47	35 37.7	117 57.9	2.9
39		5 29	0 42	7.15	35 37.3	117 54.2	3.0
40		5 7	5 16	35.19	34 57.0	118 28.7	2.7
41		4 20	10 3	47.70	35 14.5	118 58.0	2.9
42		4 3	15 0	59.00	34 52.3	119 0.1	3.3
43		3 15	3 44	57.67	35 7.0	118 29.0	2.6
44		2 6	6 28	46.81	35 12.0	118 50.3	2.9
45	'47	10 28	5 15	2.08	34 37.4	118 56.2	2.9

TABLE A-1—*Continued*

No.	Y	M	D	H	M	Sec	Lat (N)	Long (W)	M_L (M_S)
46		10	19	21	20	18.73	35° 32.8′	118° 24.8′	2.8
47		9	18	15	47	1.46	34 51.7	118 59.2	2.7
48		7	17	20	32	13.50	34 50.4	119 20.0	2.8
49		3	18	13	20	46.15	34 45.0	118 43.0	2.5
50		3	5	0	5	55.67	34 39.4	119 7.4	2.7
51		2	18	6	47	1.83	35 17.2	118 32.6	2.7
52		2	12	13	33	0.70	35 31.9	118 46.6	3.2
53		2	10	6	55	26.62	35 29.3	118 37.8	3.0
54†		2	9	5	26	8.13	34 42.0	118 47.0	2.5
55		2	7	12	19	59.46	35 28.6	118 40.8	3.1
56		2	7	6	11	51.73	35 29.8	118 31.9	2.4
57		2	3	10	11	50.41	35 3.5	118 53.5	3.0
58		2	2	0	5	38.53	35 16.8	118 32.4	2.4
59		2	1	13	30	49.42	35 17.2	118 21.7	3.5
60		2	1	11	47	26.42	35 21.4	118 13.0	2.1
61	'46	12	29	14	20	42.59	34 54.7	119 15.8	3.0
62		11	25	21	1	1.74	35 3.4	119 4.8	3.0
63		11	5	16	24	30.45	35 9.7	119 2.6	2.6
64		8	21	3	38	18.78	35 29.0	118 5.2	2.7
65				2	35	42.77	35 30.1	117 58.9	2.6
66		7	26	0	43	10.83	34 46.3	119 9.4	2.9
67		7	24	0	23	10.91	35 0.6	119 11.3	3.0
68				0	19	10.57	35 7.0	119 10.7	4.0
69		2	15	23	11	33.55	35 21.2	118 33.8	2.7
70		2	13	21	2	1.91	34 49.0	119 13.2	2.7
71		1	17	12	21	42.14	34 50.9	118 58.9	3.4
72	'45	7	25	0	8	12.58	34 54.9	118 59.6	3.3
73		7	22	2	16	37.95	35 2.4	118 52.4	2.7
74		6	16	21	37	26.01	35 0.8	118 52.2	2.7
75		3	22	5	19	0.12	35 6.9	118 52.3	2.9
76		3	15	23	34	50.30	35 50.6	119 2.4	3.0
77		2	5	21	27	12.82	35 7.6	119 2.8	2.8
78	'44	10	1	1	16	1.81	34 51.4	119 0.0	2.9
79		2	23	23	42	46.12	35 30.9	118 43.5	3.6
80	'43	10	8	3	25	1.11	34 50.3	118 56.5	2.7
81		5	24	9	21	54.52	34 36.7	118 55.3	2.5
82		4	6	22	36	25.58	34 36.7	118 55.3	2.5
83		2	17	8	32	33.04	35 2.8	118 49.0	2.6
84		1	15	18	58	30.23	35 9.9	118 58.6	2.8
85	'42	12	5	11	57	4.83	35 1.1	119 0.9	2.7
86		6	12	22	28	23.37	35 28.1	118 53.8	2.5
87		5	20	0	38	5.69	35 19.3	119 10.9	3.4
88‡	'41	9	29	15	35	12.37	35 1.5	119 16.3	3.0
89‡		9	22	2	11	58.58	34 52.0	118 49.9	3.0
90‡		9	21	23	35	18.00	34 52.0	118 56.0	3.0
91‡		9	21	20	0	36.0	34 52.0	118 56.0	3.0
92		9	21	19	53	8.61	34 52.0	118 55.9	5.2
93		3	30	23	37	6.48	35 11.4	119 15.3	3.0
94		2	9	18	53	43.46	34 50.4	119 12.8	2.5
95		1	26	14	34	22.28	34 52.6	118 54.0	3.0
96	'40	10	23	18	31	33.27	34 44.7	119 3.8	3.0
97		8	6	15	33	54.05	34 52.9	119 12.0	3.5
98		7	29	12	14	25.37	35 10.3	119 5.0	3.5
99		7	13	3	23	30.93	34 59.0	118 24.5	3.0
100		1	18	17	18	50.33	34 54.2	119 2.3	2.5
101	'39	10	25	9	45	50.23	35 0.4	119 15.3	3.0
102		10	25	9	7	30.22	34 58.8	119 14.7	3.5

TABLE A-1—*Continued*

No.	Y	M	D	H	M	Sec	Lat (N)	Long (W)	M_L (M_S)
103		9	19	4	38	29.81	34° 31.6′	118° 56.0′	3.0
104		7	24	8	41	11.66	34 56.7	119 2.6	2.5
105		7	21	16	56	27.68	35 5.0	118 18.0	3.0
106		5	8	2	48	4.28	34 58.7	119 4.0	4.5
107		4	15	5	2	36.17	34 50.0	118 55.7	2.5
108		4	7	9	25	0.44	34 40.8	118 44.6	2.5
109		3	7	19	53	31.82	34 52.8	119 1.3	4.0
110		2	23	10	25	37.10	34 50.2	119 0.0	3.5
111				9	46	0.18	35 1.5	119 3.0	3.0
112				9	33	17.79	34 55.8	119 0.0	3.5
113				9	18	47.45	34 50.9	119 1.4	4.5
114				8	58	2.91	34 54.1	119 2.6	3.0
115				8	45	50.63	35 0.5	118 59.8	4.5
116	'38	12	4	23	00	55.65	35 11.4	118 20.0	3.0
117		10	15	11	19	42.10	35 5.4	118 57.5	2.5
118		7	1	20	17	31.61	34 59.0	118 24.7	2.5
119	'37	12	19	23	36	21.61	34 49.5	118 57.5	3.0
120		10	4	8	7	47.46	35 0.0	118 53.0	2.5
121		6	9	7	58	14.24	34 38.7	119 9.1	3.0
122		4	23	3	47	48.72	35 1.0	119 8.3	2.5
123†	'36	12	22	9	17	47.90	34 53.0	116 52.9	2.5
124		12	1	4	36	31.00	34 52.5	119 17.6	3.0
125		11	29	5	54	45.63	34 53.8	119 1.8	3.8
126		10	10	6	17	33.42	35 14.4	118 47.7	3.0
127		10	5	22	50	21.07	35 2.7	118 53.1	3.5
128		9	27	1	55	40.44	35 24.1	118 54.3	3.5
129		8	21	5	12	13.43	35 4.9	118 52.2	2.7
130		8	4	8	1	37.34	35 0.0	119 2.2	3.0
131		5	31	4	41	53.95	35 4.6	119 4.8	2.9
132		3	24	4	2	22.76	35 22.6	118 35.6	2.5
133	'35	11	23	15	58	4.71	35 4.6	119 18.7	2.5
134		10	27	16	9	24.13	34 46.7	118 54.2	2.5
135		9	20	9	14	37.81	35 11.0	118 17.5	2.0
136		9	10	21	27	1.36	35 11.3	119 15.4	3.0
137		7	7	23	01	1.03	35 6.1	118 56.7	2.9
138		6	11	18	10	51.63	34 54.8	118 59.8	4.0
139		4	14	6	59	8.75	35 5.1	118 53.0	2.5
140				6	52	10.46	35 3.8	118 56.8	2.6
141		3	18	14	57	27.06	35 22.7	118 50.0	2.5
142		3	17	20	26	49.95	35 23.1	118 47.8	4.0
143		3	5	12	45	39.93	35 17.4	118 17.6	2.5
144		3	4	23	54	49.81	35 14.6	118 23.0	2.7
145	'34	12	21	9	28	3.21	34 51.8	118 40.9	2.0
146		12	6	7	43	31.54	35 13.1	118 56.8	3.7
147		11	17	1	25	46.25	35 24.1	118 47.7	2.5
148		10	13	14	6	11.16	35 9.4	119 7.4	2.5
149		9	28	7	28	29.25	34 59.0	118 24.5	2.0
150		7	13	6	32	24.45	35 6.6	118 30.2	2.5
151		7	6	23	57	15.96	35 15.6	118 10.9	2.0
152	'33	11	20	7	39	47.36	34 29.9	118 58.9	3.0
153		10	15	14	1	38.88	35 23.2	119 7.9	2.8
154		9	4	8	13	55.87	35 6.1	118 11.9	3.0
155	'32	12	3	21	39	40.31	34 28.9	119 10.0	3.0
156		11	26	7	15	48.66	34 50.9	118 56.4	2.7
157		10	25	12	50	12.85	34 39.4	118 45.0	3.5
158		9	24	9	22	9.67	35 17.3	117 48.7	2.0

TABLE A-1—*Continued*

No.	Y	M	D	H	M	Sec	Lat (N)	Long (W)	M_L (M_S)
159§		7	30	23	16	7.4	34° 43.0′	119° 3.0′	2.5
160§		7	25	21	33	4.5	34 53.0	119 0.0	2.0
161§		6	23	7	25	30.5	34 55.0	119 5.0	2.5
162§		6	2	12	56	5.9	34 40.0	118 50.0	2.0
163†		2	14	17	55	18.79	34 18.3	119 0.0	2.5

* Original seismograms reread.

† Very large residual and location questionable.

‡ Insufficient data, not relocated.

§ Phase cards missing, not relocated.